Enabling safe and stable Li metal batteries with protic ionic liquid electrolytes and high voltage cathodes

Enabling safe and stable Li metal batteries with protic ionic liquid electrolytes and high voltage cathodes

Gabriele Lingua[a], Marisa Falco[a], Timo Stettner[b], Claudio Gerbaldi[a,*], Andrea Balducci[b,*]

[a] GAME Lab, Department of Applied Science and Technology (DISAT), Politecnico di Torino, C.so Duca degli Abruzzi 24, 10129, Torino, Italy.

[b] Friedrich-Schiller-University Jena, Institute for Technical Chemistry and Environmental Chemistry, Center for Energy and Environmental Chemistry Jena (CEEC Jena), Philosophenweg 7a, 07743, Jena, Germany

* Corresponding Authors: claudio.gerbaldi@polito.it; andrea.balducci@uni-jena.de

Abstract

Here, we present first examples of lithium metal cells stable and safely operating with $PYR_{H4}^{+}(TFSI^{-}/FSI^{-})$-based protic ionic liquid (PIL) electrolytes, which is accomplished by encompassing vinylene carbonate (VC) in the PIL-salt solution. VC not only enhances the stability window of PIL electrolytes; it also undergoes electrochemical decomposition during initial cycling, thus creating a protective barrier at the electrolyte/electrode interface. The protective film prevents degradation at the Li metal anode due to hydrogen release, as well as at the cathode side at anodic potential. Materials and related devices are investigated in their main physico-chemical characteristics, ionic conductivity, electrochemical behavior by impedance spectroscopy, cyclic voltammetry and galvanostatic cycling. Newly designed electrolyte formulations enable direct cycling of Li-metal cells with PILs to achieve excellent stability with LFP and NMC-based cathodes, almost full capacity (≥160 $mAhg^{-1}$) and highly reversible operation at RT and different current rates up to 1C. The PIL-VC based cell outperforms bare PIL electrolyte as well as the aprotic $PYR_{14}TFSI$ based cells, thus enlightening a feasible strategy to suppress the high reactivity of PILs towards alkali metals; along with the use of appropriate materials, this may turn high energy density, low-cost PIL-based Li-metal batteries into industrial reality soon.

Keywords: protic ionic liquid; vinylene carbonate; lithium battery; lithium metal protection; high voltage cathode

1. Introduction

In the forthcoming decade, the growth in electrification of modern society will mainly be driven by the irreversible deployment towards decarbonization in many critical sectors: large investments for the exploitation of renewable energy resources are increasing worldwide, with particular attention to wind and solar power energy plants, which are the most mature technologies [1]. In this scenario, batteries are identified as high-performance systems that can efficiently store and deliver energy on demand along with reducing the carbon footprint of the transportation sector, stabilize the power grid and support a wide range of strategic industries [2]. Lithium-ion batteries (LIBs) are nowadays one of the most important energy storage devices. LIBs are already dominating the portable consumer electronic market and have been indicated as the most promising electrochemical devices for the realization of hybrid-electric, plug-in and full electric vehicles, as well as for advanced delocalized energy storage units [3]. The commercially available LIBs contain electrolytes based on organic carbonate mixtures (e.g., ethylene carbonate - EC, and diethyl or dimethyl carbonate - DEC/DMC). These electrolytes show high ionic conductivity, excellent wetting properties and low charge-transfer resistance at the interface with the active materials [4]. However, the presence of flammable and volatile organic solvents accounts for serious safety hazards, including leakage, auto-combustion and/or explosion in abusive conditions [5]; these features are also accompanied by serious environmental issues, such as pollution of soil/water sources and human health, especially at the end of a battery life without proper recycling/remanufacturing [6].

These issues are prompting research on the development of new electrolyte materials. In this scenario, ionic liquids (ILs) are considered amongst the most promising candidates to replace conventional organic liquid electrolytes [7]. ILs are an interesting class of salts having melting points lower than 100 °C, with major advantages over organic solvents, which include negligible vapour pressure at low/moderate temperature, high chemical and thermal stability, and, in some cases, hydrophobicity; as a result, they are considered safe due to non-flammability, and they have also attracted great attention for use as “green” solvents for chemical reactions [8,9],[10].

Synthesis procedures of several families of aprotic ILs (AILs) have already been deeply studied and optimized [11–13], as well as their energy application as electrolytes or electrolyte components for electrochemical devices - including rechargeable batteries, fuel cells, double-layer capacitors and hybrid supercapacitors - due to their high ionic conductivity and electrochemical stability [14–19]. Nevertheless, a subset family of ILs, called protic ionic liquids (PILs), is receiving increasing attention in recent years, as they possess all the attractive features of AILs, but, in addition, they are typically cheaper and easier to prepare, thus more sustainable [20,21]. PILs are synthesized via direct neutralization reactions of a Brønsted acid (proton donor) and a Brønsted base (proton acceptor) [14], resulting in most cases in a nitrogen-containing organic cation singly or doubly protonated with a corresponding counter anion. The main advantage of PILs over AILs results from the presence of less shielded cations in the former ones, intrinsically responsible for the "cation competition effect", which, in a mixture of PIL-Li salts, results in loosely coordinated Li^+ ions along with improved mobility [22,23].

The use of PILs as electrolytes in LIBs is rather recent [24], and their use in high-energy Li metal battery has never been considered so far because of the presence of acidic protons, which are strongly reactive towards the Li metal electrode. It is well known that Li metal is the ultimate choice for the anode amongst all possible candidates, because it has the highest theoretical capacity (3,860 mAh g^{-1}) and lowest electrochemical potential (–3.04 V *vs.* the standard hydrogen electrode) [3,25,26],[27]. Furthermore, the Li metal anode is the core of Li-S and Li-air systems, both of which are being intensively studied for next-generation energy-storage applications [28], as well as the intriguing opportunity of reaching the maximum energy density achievable by Li metal cells operating with high voltage cathodes (e.g., LMNO, $LiCoPO_4$, NMC at very low Co content or Li-rich NMC) [29],[30]. Therefore, the combination of PILs as electrolyte components with Li metal anode is still a great challenge, possibly leading to high-energy density devices, with improved performances compared to the systems with AILs, mostly due to the enhanced mobility of Li^+. Considering all the above mentioned attractive features of PILs, the introduction of this(these) innovative electrolyte(s) could be of importance for the development of safe and cheaper IL-based Li-metal batteries, thus establishing new market opportunities.

In this work, we report for the first time the use of pyrrolidinium-based PILs with Li metal as anode in two different lithium ion battery configurations, using both lithium iron phosphate (LFP) and lithium nickel manganese cobalt oxide (NMC) as cathodes. The electrolytes consist of solutions of N-butylpyrrolidinium-bis(trifluoromethanesulfonyl)imide ($PYR_{H4}TFSI$) or N-butylpyrrolidinium-bis(fluoromethanesulfonyl)imide ($PYR_{H4}FSI$) in combination with lithium bis(trifluoromethanesulfonyl)imide (LiTFSI) or lithium bis(fluoromethanesulfonyl)imide (LiFSI), respectively. The electrolyte solutions are combined with vinylene carbonate (VC) that has the fundamental purpose of promoting the formation of a thin protective layer on the Li metal anode, preventing detrimental reactions due to the protic ILs, by means of electrochemically induced reductive decomposition upon initial cycling [31],[32]. Within this work, remarkably stable ambient temperature cycling at different current regimes is firstly demonstrated even with > 4 V class NMC composite cathodes, as well as in comparison with the corresponding AIL based cells.

2. Experimental

2.1 Synthesis of protic ionic liquids (PILs) and PIL-based electrolyte solutions

N-butylpyrrolidinium-bis(trifluoromethanesulfonyl)imide ($PYR_{H4}TFSI$) and N-butylpyrrolidinium-bis(fluoromethanesulfonyl)imide ($PYR_{H4}FSI$) were synthesized following similar procedures described elsewhere [14,33]. In a first step, the yellowish precursor 1-butylpyrrolidine (98 %, obtained by *Aldrich*) was distilled at 60 °C and 20 mbar. After the distillation, the resulting colorless 1-butylpyrrolidine (25 mmol) was put in a two-neck flask equipped with a magnetic stirrer and a dropping funnel filled with 5.35 ml of HCl (35 %), topped by a reflux condenser. The reaction flask was placed in an ice bath and HCl (in molar excess) was added dropwise under continuous stirring. After the addition, the ice bath was removed and the solution was stirred for two hours at ambient tempearature. Residual water and reactants were removed under reduced pressure, leaving 1-butylpyrrolidine-chloride as a solid.

The 1-butylpyrrolidine chloride (25 mmol) was dissolved in 8 ml of H_2O and then put in to a two-neck flask equipped with the same setup used for the first synsthesis step. In order to get the final TFSI and FSI PILs, equimolar amounts of LiTFSI (99.95 %, from *Aldrich,* now *Merck*) or LiFSI (99.95 %, from *Aldrich,* now *Merck*),

respectively, were dissolved in 18 ml of H_2O and filled into the dropping funnel. In both cases, the lithium salt solution was added dropwise to the 1-butylpyrrolidine chloride solution while keeping stirring. The solution was stirred for 3 hours to ensure complete anion exchange. At the end of the reaction, a separating funnel was used to remove the aqueous phase from the organic one. Subsequently, the protic ionic liquids were washed six times with water, to remove residual LiCl. To test on complete removal, $AgNO_3$ was added to the washing water. LiCl reacts with $AgNO_3$ to AgCl, which is poorly soluble, so the absence of a precipitation confirms the complete removal of LiCl. As a last step, residual water was removed by reduced pressure and heating (60 °C, $3.0x10^{-3}$ mbar).

In an Ar-filled dry glove box (MBraun UniLab, O_2 and H_2O < 1 ppm), two liquid electrolyte solutions were prepared, hereafter named H_4TFSI and H_4FSI, consisting in LiTFSI or LiFSI (both battery-grade, from *Solvionic*, vacuum-dried at 150 °C for 48 h, and at 70 °C for 24 h before use, respectively) dissolved in Pyr_{H4}TFSI or Pyr_{H4}FSI PILs (vacuum-dried at 60 °C for 48 h) to obtain one fully $TFSI^-$ and one fully FSI^- anion based solution, respectively. In both cases, the molar ratio between the PIL and the corresponding Li salt is 4:1, which was selected, being the one with highest lithium salt concentration without crystalline phase formation, avoiding detrimental effect to battery cycling [34].

The solutions were stirred for several hours at 30 °C until complete salt dissolution. A portion of each of the above mentioned solutions was added with 10 wt% of vinylene carbonate - VC (battery grade, *Solvionic*, used as received), followed by stirring to ensure homogeneity of the resulting solutions, hereafter named H_4TFSI-VC and H_4FSI-VC. The four PIL-based electrolyte solutions were safely stored in the dry glove box.

2.2 Characterisation techniques

The ionic conductivity of the electrolytes was measured using a potentiostat *ModuLabXM* (*Solartron analytical*) in the temperature range between −30 and 80 °C. The samples were placed in sealed cells with Pt plated electrodes. The conductivity values were calculated from the dielectric measurements following the method reported by Leys et al. [35]. Cells for conductivity tests feature platinum plated electrodes and were filled with the electrolyte under argon atmosphere. Impedance spectroscopy was carried out in the frequency

range of 300 KHz to 1 Hz, with an alternating current of 5 mV, to measure the resistance. The viscosity of the electrolytes was determined using a rheometer *MCR 102* (*Anton Paar*), starting with shear rate of 500 s^{-1} for the analysis at 10 °C and progressively increasing it by 250 s^{-1} for each 10 °C step in the temperature range between 10 and 80 °C. The density of the electrolytes was determined in the temperature range between 20 and 80 °C, using the density meter *DMA 4100M* (*Anton Paar*).

The electrochemical stability window (ESW) was measured in a three-electrode cell with a Pt working electrode (WE), an oversized carbon counter electrode (CE), and an Ag quasireference electrode (QRE). After 12 hours of equilibration at the open circuit voltage (OCV), the potential was linearly varied to -3 V or 3 V *vs*. Ag QRE with a scan rate of 1 mV s^{-1}. The ESW was also evaluated in Li-metal cells, with lithium metal as both counter and quasireference electrode, using a steel (SS-316) EL-cell. A *Whatman* glass wool disk, previously soaked with PIL electrolyte solution, was sandwiched between the two electrodes, namely copper foil and a lithium metal disk. The potential was linearly swept from OCV to 0.3 V *vs*. Li^+/Li with a scan rate of 0.1 mV s^{-1}. Fresh electrolyte was used for the anodic and the cathodic sweeps, respectively.

The Li plating/stripping experiments were carried out using two-electrode *Swagelok* cells equipped with Li metal electrodes. *Whatman* glass microfiber filters (150 µm) were used as separators drenched with 150 µL of electrolyte. The cells were assembled under Ar-atmosphere in a *MBraun LABmasterpro ECO glove box* (O_2 and H_2O < 1 ppm). Galvanostatic cycling (GC) tests were performed at 25 °C at a fixed current density of 0.088 mA cm^{-2} (0.1 mA current, 1.13 cm^2 electrode area), with plating or stripping steps lasting for different times (i.e., 30, 90 and 150 min).

2.3 Electrode/cell preparation and electrochemical testing

The electrochemical performance of the liquid electrolytes in lab-scale Li metal cells was evaluated by means of charge/discharge GC with both $LiFePO_4$ (LFP) and $LiNiMnCoO_2$ (NMC) based electrodes. *Whatman* GF/A glass wool disks were used as separators drenched with 200 µL of electrolyte. The composition of the LFP composite electrodes was 80 wt% of the active material LFP ($LiFePO_4$+C, Life Power® P2, *BASF*), 12 wt% of the electrically conductive agent (carbon black C-NERGY™ Super C65) and 8 wt% of poly(vinylidenefuoride) -

PVdF (Solvay *Solef 2010*) as the binder, while the composition of the NMC composite electrodes was 94 % of the active material NMC (Ni:Mn:Co = 6:2:2, *BASF*), 3 % of the electrically conductive agent C65 and 3 wt% of PVDF as the binder. The following procedure was adopted for all the electrode preparations. First, powders of active material and C65 were gently mixed in a hand mortar. Successively, the mixture was added to a solution of PVdF in ≈1 ml of N-methyl pyrrolidone (NMP, *Aldrich*, now *Merck*) under constant stirring, which was continued for 3-4 h at ambient laboratory temperature (i.e., ≈21 °C). The resulting dense, homogeneous slurry was casted onto an Al current collector using a doctor-blade. NMP solvent was removed by evaporation at ambient temperature and further drying at 60 °C / vacuum for 24 h prior to utilization. The average active material mass loadings were 5 and 6 mg cm^{-2} for the LFP- and the NMC- based electrodes, respectively, with thickness values in the range of 50-60 µm. The lab-scale cells were cycled at ambient laboratory temperature at different current-rates, where the rate denoted as C/n corresponds to a full discharge (or a full charge) in n hours, based on the theoretical cathode capacity (C) of the corresponding electrode material. The lab-scale Li/PIL-based electrolyte/LFP cells were cycled between 2.7 and 3.7 V *vs.* Li^+/Li, while the Li/PIL-based electrolyte/NMC cells between 3.0 and 4.3 V *vs.* Li^+/Li, where the Li metal was used as both CE and reference electrodes. The electrochemical tests described above were performed using a *VMP3* electrochemical workstation (20 V, ±400 mA) by *BioLogic Science Instruments* (France) using *ECC-Std test cells* (*EL-Cell GmbH*, Germany). Test cells were assembled inside the Ar-filled glove box to avoid moisture contamination.

3. Results and discussion

Fig. 1 shows the comparison of viscosity (1a) and conductivity (1b) of the two PIL-based electrolytes investigated in this work: H_4TFSI-VC and H_4FSI-VC. At 30 °C, the TFSI-based electrolyte displays a viscosity of 38 mPa s, while the viscosity of the FSI-based electrolytes is 27 mPa s. Just for comparison, these values are lower than those displayed by the neat ILs at the same temperature (43 mPa s for Pyr_{H4}TFSI and 30 mPa s for Pyr_{H4}FSI) [36,37], which is most likely due to the presence of VC. The significant difference between the viscosity of H_4FSI-VC (39 mPa s) and that of H_4TFSI-VC (60 mPa s) at 20 °C might be related to the proximity of the melting point of crystalline Pyr_{H4}TFSI [38]. At higher temperature (80 °C), the two electrolytes display

comparable viscosity values (9 and 11 mPa s for H_4FSI-VC and H_4TFSI-VC, respectively). As shown in **Fig. 1b**, the ionic conductivity of the H_4FSI-VC is higher than that of the H_4TFSI-VC over the entire temperature range investigated. This trend it is not surprising considering that H_4FSI-VC displays viscosity values lower than those of H_4TFSI-VC in the same temperature range. This is commonly observed when comparing ILs with $TFSI^-$ vs. their counterparts with FSI^-, due to the anion size [37]. Accordingly, the difference in conductivity is more marked at lower temperature: at 20 °C the FSI-based electrolyte is displaying a conductivity of 5.5 mS cm^{-1}, while the TFSI-based one a value of 1.9 mS cm^{-1}. It is also noticed that although the viscosities of the investigated PIL-based electrolytes are lower compared to their neat counterparts, the conductivity of the former ones is lower (e.g., at 30 °C, 8.6 mS cm^{-1} for Pyr_{H4}FSI *vs.* 7.7 mS cm^{-1} for H_4FSI-VC and 4.0 mS cm^{-1} for Pyr_{H4}TFSI *vs.* 3.0 mS cm^{-1} for H_4TFSI-VC) [39]. This observation can be explained considering that the introduction of lithium salt increases the amount of charge carriers, thus increasing the recombination of ions in the system and lowering the overall conductivity. Nevertheless, it has already been shown, that the mobility of Li^+-ions is rather high in protic ionic liquids, especially compared to that in their aprotic counterparts [22]. Lastly, an important part of the charge transport in these electrolytes is performed by the protons of the PILs. It has been demonstrated that PILs might be able to form a hydrogen-bonded network, which allows H^+ migration through structural diffusion (the "Grotthuss mechanism") [40,41]. However, since the conductivity of the electrolytes under study is not increasing drastically compared to their viscosities, in this case, conventional vehicular charge transport is likely to be the dominant process.

As shown in **Fig. S1** (Supplementary Data), the variation of density over temperature displays a comparable linear trend for both H_4TFSI-VC and H_4FSI-VC. Also in this case, the difference between the two electrolytes is related to the nature of the anion counterpart. At 30 °C, the FSI-based electrolyte shows a density of 1.37 g cm^{-3}, while the density of the TFSI-based electrolyte is 1.45 g cm^{-3}; moreover, both electrolytes are denser compared to their pure counterparts.

As mentioned in the introduction, the electrochemical stability window (ESW) of PILs is limited by the presence of the labile proton(s) in the cation structure. Specifically, the cathodic potential limit is considerably reduced compared to that of their aprotic counterparts.

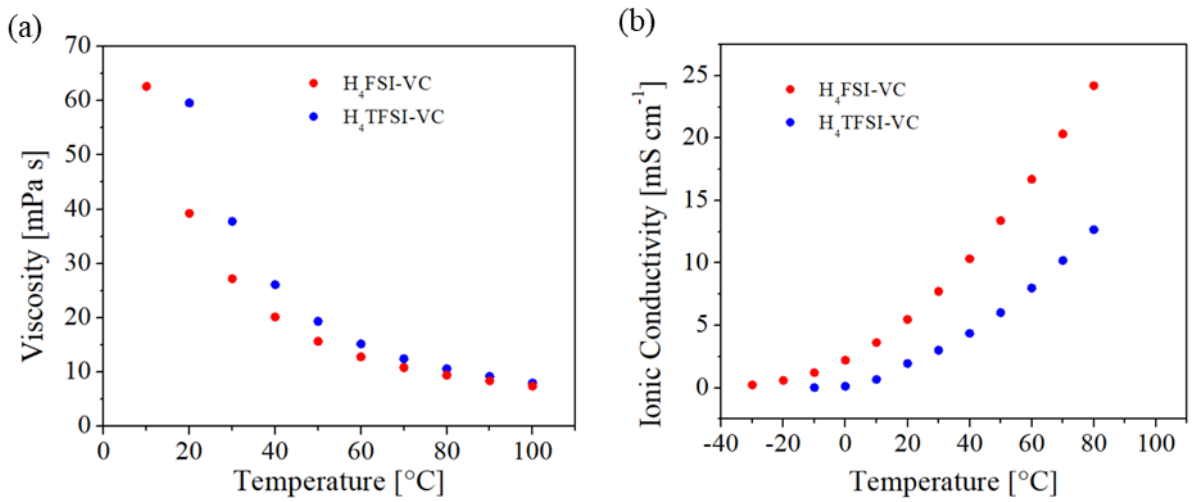

Figure 1. Influence of the temperature on the (a) viscosity and (b) conductivity of the investigated PIL-based electrolytes.

On the other hand, it has been already shown that the anodic stability window (ASW) of PILs is almost analogous to that of AILs having the same anion [42]. Neat $Pyr_{H4}TFSI$ and $Pyr_{H4}FSI$ show comparable cathodic potential limits, close to -1 V *vs.* Ag QRE while, in terms of anodic potential limit, the FSI-based PIL results to be less stable towards oxidation due to the higher chemical and electrochemical reactivity of the former compared to the latter anion. Similar behaviour has been observed before [43]. The comparison of **Fig. 2(a,b)** clearly shows that the addition of VC leads to a variation of ASW of the two PIL electrolytes. It seems that the oxidation process of VC, at *ca.* 4.6 V vs Li^+/Li [44], prevails over the other oxidation mechanisms, defining the oxidation potential limits for H_4TFSI-VC and H_4FSI-VC. In addition, the presence of VC leads to a notable improvement of the cathodic stability window (CSW) in both electrolytes. As shown in the **Fig. 2b** (and in the magnification reported in Fig. S2 in Supplementary Data), both of them are stable till –2.9 V *vs.* Ag QRE (corresponding to *ca.* 0 V *vs.* Li^+/Li, which is the potential at which lithium plating takes place). The cathodic potential limit results to be *ca.* 2V higher compared to the neat PIL one, indicating clearly that the presence of VC, through a polymerization/decomposition process, leads to obtain a protective layer on the Li metal surface, likely preventing the direct contact between Li metal and PIL [31],[44]. In order to get further information about the electrochemical reduction of VC, the CSW was also evaluated in a Li/H_4FSI-VC/Cu cell with a Li metal electrode as the reference. The easily detectable reduction process occurring in the voltage

range between 1.5-2 V vs. Li QRE (insert of **Fig. S3** in Supplementary Data) can be assigned to the electrochemical reduction (polymerization) of VC.

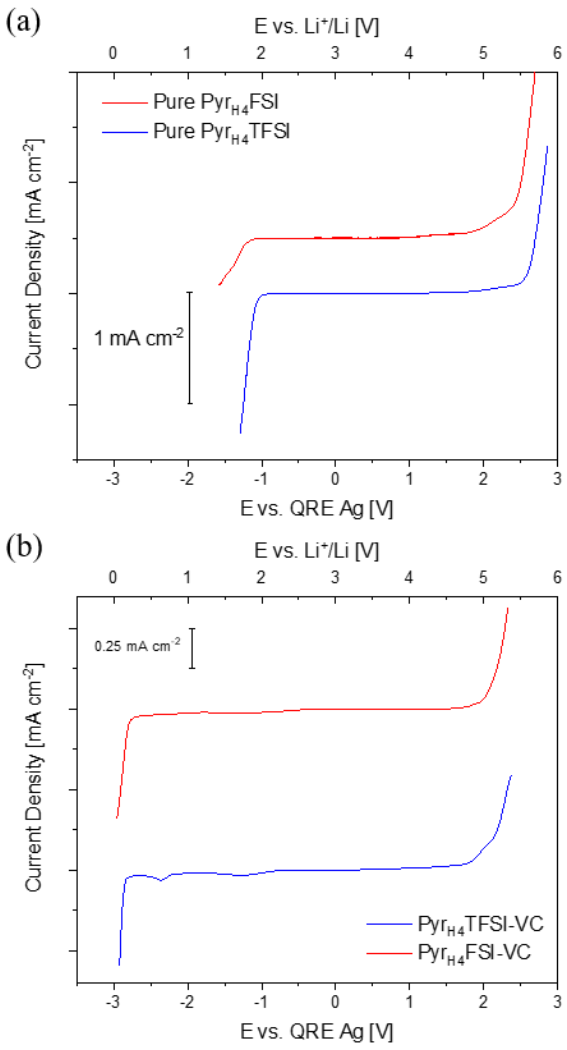

Figure 2. Electrochemical stability window of: (a) pure $Pyr_{H4}FSI$ and $Pyr_{H4}TFSI$; (b) H_4TFSI-VC and H_4FSI-VC electrolytes.

In general, this process occurs at relatively high potential values as compared to the other components in the common electrolytes [31],[45], promoting the formation of a passivation layer, which prevents detrimental reactions due to $[Pyr_{H4}]^+$ at the Li-metal anode.

To further investigate the compatibility of the PIL-based electrolytes with the Li metal electrode, Li plating/stripping experiments were also carried out. **Fig. 3(a,b)** show the voltage profiles of Li metal symmetrical cells, using H_4FSI-VC and H_4TFSI-VC solutions as electrolytes.

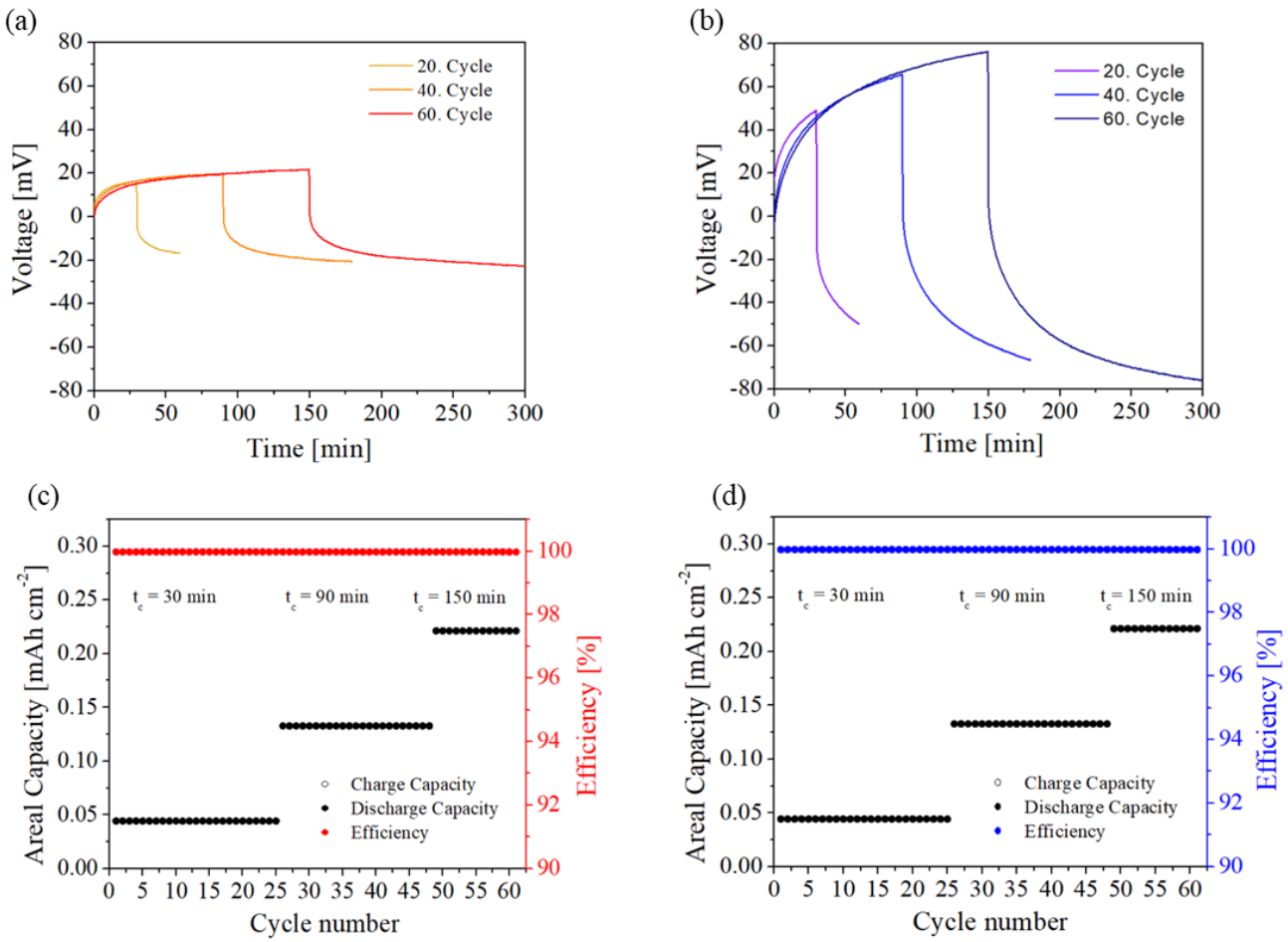

Figure 3. Voltage profiles of symmetrical Li metal cells in combination with (a) H_4FSI-LiFSI-VC and (b) H_4TFSI-LiTFSI-VC as electrolyte, as well as the results of charge-discharge measurements of (c) H_4FSI-LiFSI-VC/Li and (d) H_4FSI-LiFSI-VC/Li, all at different charge times. The experiment was conducted at 25 °C and the current density of 0.088 mA cm^{-2}.

The plating/stripping profile of the H_4FSI-VC sample is characterized by relatively limited overpotential (± ≈ 15-20 mV) and flatter outline when compared with the TFSI counterpart (± ≈ 50-80 mV). This behavior could be imputed to the intrinsic properties of FSI^--based electrolytes. **Fig. S4** shows the poor reversibility of the lithium plating/stripping process without VC addition, corresponding to a severe increase of cell overpotential and capacity fade from the early cycles.

The lower viscosity, higher conductivity and the capacity of forming a more stable solid electrolyte interface (SEI) make lithium ion diffusion and plating/stripping processes easier with FSI^- anion [46]. **Fig. S5** in supplementary data clearly demonstrates the better film forming ability of FSI-based electrolytes, limiting the increase of the electrolyte bulk resistance during the plating/stripping process, which could be directly

correlated to the reduced overpotential. Nevertheless, both cells appear to be stable even during prolonged constant-current plating/stripping steps; in fact, no sign of severe electrolyte degradation was observed, both in terms of overpotential (cell resistance) and coulombic efficiency (reversibility). **Fig. 3(c,d)** show stable cycling up to 60 cycles with each step lasting for 150 min, along with high (> 99.9 %) efficiency during the whole measurement. The plating/stripping analysis underlines the beneficial effect of VC when added into the electrolyte solution, effectively limiting decomposition reactions of the PILs after prolonged contact with Li metal, and accounting for the excellent lithium plating/stripping ability in PIL-based electrolytes.

Fig. 4(a,b) clearly show the difference in the galvanostatic behaviour of Li/PIL-based electrolyte/LFP cells with and without VC. As evident in **Fig. 4a**, the use of PIL-based electrolyte in direct contact with the Li metal electrode leads to rapid cell failure in about five cycles. Actually, the acidic proton strongly affects the reactivity of PILs towards alkali metal electrodes, making them extremely more reactive than their aprotic counterparts [47]. This reactivity is presently hindering the use of PIL-based electrolytes in alkali metal batteries, limiting the field of application of this family of electrolytes. The high irreversible capacity of the first cycle clearly accounts for side reactions, including the deprotonation of the pyrrolidinium cation resulting in H_2 evolution and PIL degradation. The presence of VC was found to be fundamental to allow cycling with Li metal anode, as shown in **Fig. 4b**. The Li/H_4TFSI-VC/LFP cell shows the typical flat plateaus of LFP cathode material for the first cycles, corresponding to Li^+ ion deinsertion (charge) and insertion (discharge) from/in the $LiFePO_4/FePO_4$. The Li metal cell assembled with H_4TFSI-VC is able to deliver 170 mAh g^{-1} during the first cycle at C/20 and 120 mAh g^{-1} at C/10, with high reversibility (Coulombic efficiency - CE approaching 100% during the whole cycling test) and a remarkably improved capacity retention (≈ 75 % after 50 cycles) as compared to the VC-free cell. To our knowledge, in addition of being remarkable, this is the first result of this kind with a liquid PIL-based electrolyte.

These excellent results can be only explained considering the decomposition/polymerization of vinylene carbonate occurring during the first charge, resulting in the formation of a protective film onto the Li metal electrode. Similar to other alkyl carbonates, VC is also reduced to species containing $–OCO_2Li$ groups, part of which may also have C=C double bonds. However, in contrast to the commonly used alkyl carbonate solvents the reduction of VC probably forms polymeric chains by reactions of the double bond through radical

polymerization [31]. The polymerization of VC at the surface of the Li metal electrode during the first reduction process occurring at the Li metal anode affects the surface chemistry of the electrode, reducing the irreversible capacity and suppressing the rapid electrolyte degradation, making the use of PILs with Li metal anode possible. It also accounts for a very stable passivation film onto the Li metal electrode; actually, it can constantly sustain the volumetric variation of the lithium electrodes, which normally induces significant mechanical stress on the SEI leading to the formation of cracks and exposing fresh-lithium directly to the electrolyte.

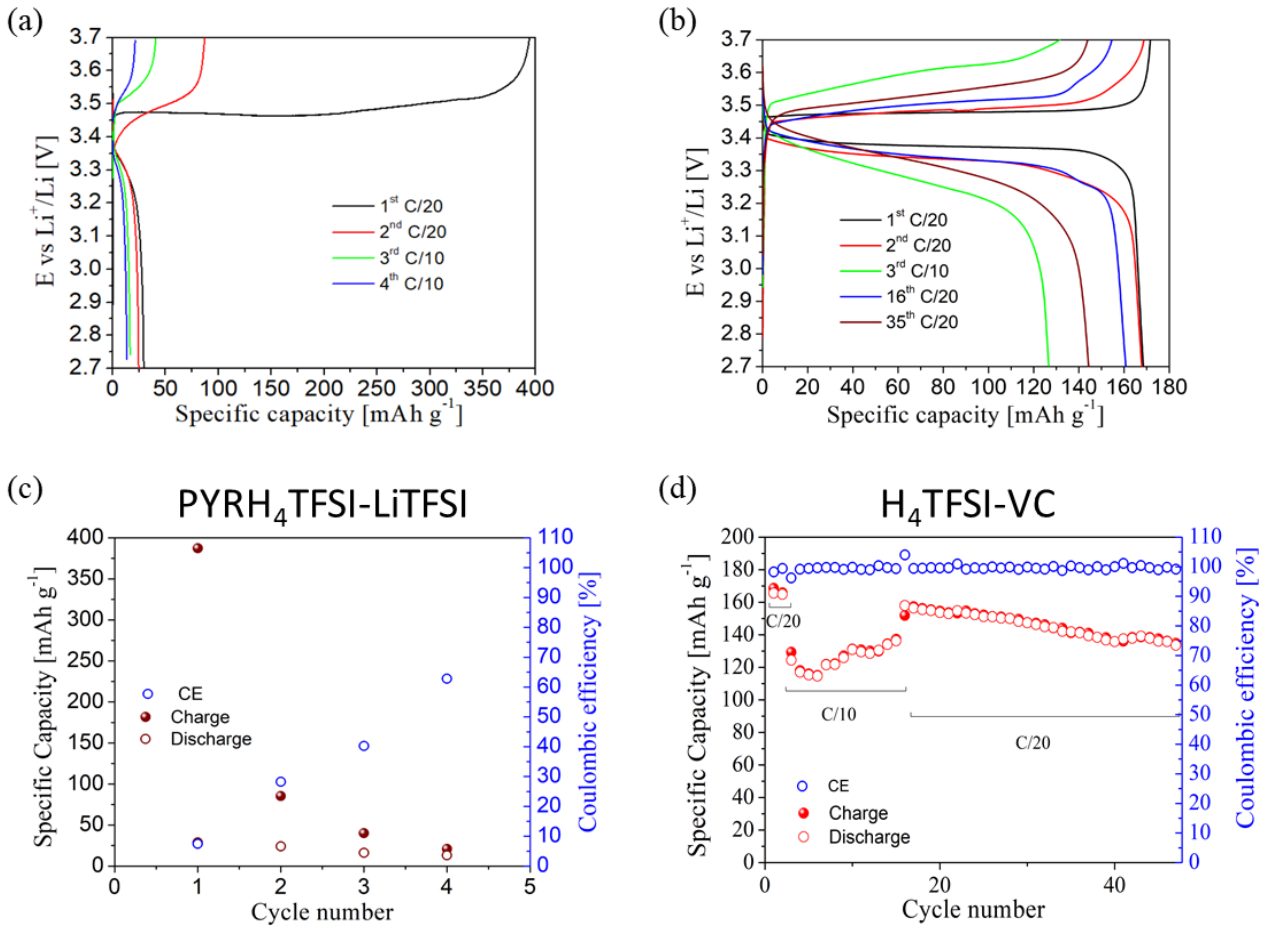

Figure 4. Galvanostatic charge/discharge cycling behavior of [Li metal/PIL-based electrolyte/LFP] cells assembled with PYR_{H4}TFSI-LiTFSI and H_4TFSI-VC PIL-based electrolytes, respectively: voltage *vs.* specific capacity profiles at different C rates and evolution of the specific capacity (a,b) and specific charge/discharge capacity and coulombic efficiency vs. cycle number at C/10 and C/20 rates (c,d). All of the measurements were performed at ambient laboratory temperature (≈21 °C), setting the same C rate for both the charge and discharge steps.

In our system, we can even assume that the bare new, free, exposed lithium metal surface that might form upon cycling almost completely reacts again with the excess of VC, to form a new SEI in equilibrium with the peculiar polarization conditions that the electrode is experiencing [48,49], thus accounting for the limited capacity fade upon cycling. The stability and robustness of the protective layer upon cycling at higher current regimes was confirmed by reducing the current rate again to C/20 after the 15th cycle: the cell recovered almost 95% of the initial discharge specific capacity. The rather consistent capacity drop while doubling the current rate to C/10 likely accounts for the rather low Li^+ ion diffusion/mobility throughout the VC-based protective film formed; further optimisation is needed in this respect, in particular considering the effect of the PIL anion and electrolyte formulation.

Motivated by the promising results discussed above, obtained with standard LFP-based electrodes operating at moderate voltages and well in the stability range of common LIB electrolytes, the performance of H_4TFSI-VC was assessed in lab-scale Li metal cell using high voltage NMC-based composite cathodes. Primary advantages of NMC-based LIBs are their high energy density and stability, allowing devices to be lighter and more compact, more durable and better to manage. Actually, the upper voltage limit for NMC is around 4.2 V vs. Li^+/Li, much higher than the LFP, which is around 3.5 V vs. Li^+/Li. If the capacities of the batteries remain constant, the energy content is defined by the voltage, which turns NMC to be a material suitable to build much higher energy density batteries compared to LFP, particularly when combined with the lithium metal anode.

Similarly to the LFP-based cell operating with the fully TFSI-based PIL/VC-based mixture, the discharge voltage profile is stable and reproducible upon initial cycling, but the Coulombic efficiency decreases quickly from the 9th cycle (see **Fig. S6** in Supplementary Data). These drawbacks, probably related to the $TFSI^-$ anion, can be to a large extent improved employing a solution based of FSI^- anion, considering the remarkable performance in terms of anodic stability and more stable SEI formation [50]. Future work is needed to confirm wether this poor cycling ability is to be attributed to the $TFSI^-$ anion or to the quantity of VC in the system.

Taking these results into account, and in order to enhance the electrochemical performance of the NMC/Li cell with PIL-based electrolyte, we investigated its behaviour in combination with H_4FSI-VC. **Fig. 5a** shows the typical charge/discharge profiles of an NMC cathode in a Li metal cell with the configuration Li/H_4FSI-VC/NMC

at different charge/discharge rates up to 1C in the voltage range of 3.0-4.3 V *vs.* Li^+/Li. The specific capacity delivered by the cell exceeded 155 mAh g^{-1} during the initial cycles at C/20 rate, which is fundamental for proper initial activation of this cathode material. The capacity drop while doubling the current rate at C/10 was actually very limited and the cell still delivered more than 145 mAh g^{-1} (15^{th} cycle), 130 mAh g^{-1} (20^{th} cycle) at C/5, 85 mAh g^{-1} (30^{th} cycle) at C/2 and above 50 mAh g^{-1} (40^{th} cycle) even at C/5. In addition, reversible charge discharge behavior was observed throughout 60 cycles, suggesting that the FSI-based electrolyte solution allows relatively stable operation with NMC cathodes, as shown in **Fig. 5b**. Except for cycling at a high current rate of 1C, the coulombic efficiency was stable above 99 % during the whole test. The specific capacity was almost completely restored when the current rate was lowered back to C/10 (capacity retion of 95 %), with no straightforward (≈ 8 %) fading even after 60 cycles. At present, we may ascribe what we observed to a better (improved compared to $TFSI^-$) and stable passivating layer at the interface of Li metal to effectively prevent its contact with the electrolyte solution that may cause the deterioration of the performance upon prolonged cycling.

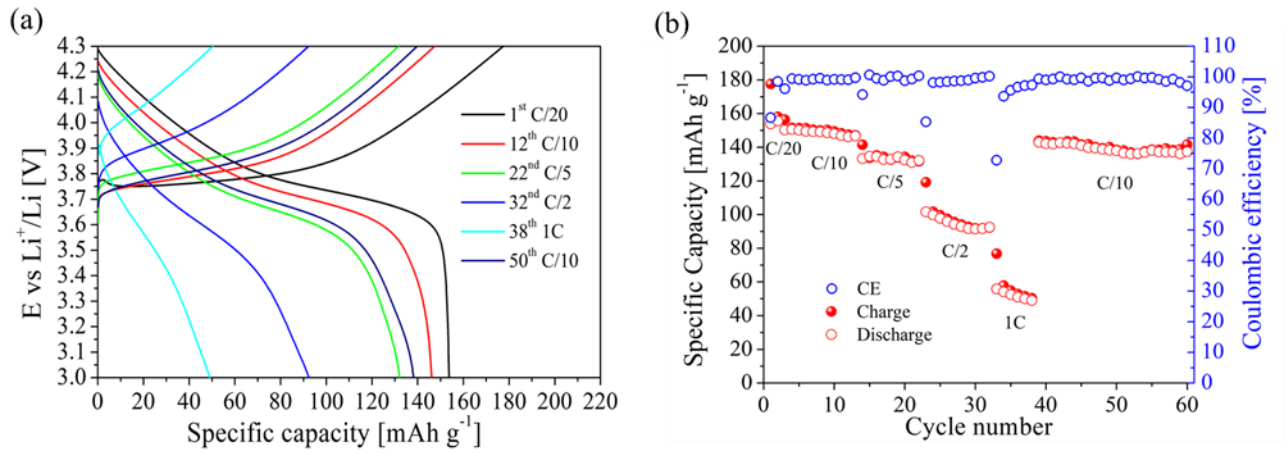

Figure 5. Galvanostatic charge/discharge cycling behavior of [Li metal/H_4FSI-VC/NMC] cells: voltage vs specific capacity profiles at different C rates (a) and evolution of the specific capacity and the Coulombic efficiency with the cycle number (b). All of the measurements were performed at ambient laboratory temperature (≈21 °C), setting the same C rate for both the charge and discharge steps.

In our case, with sufficiently high concentration of VC present in the electrolyte, residual VC likely remains in the electrolyte after anode SEI formation, which may undergo oxidation at the interface between electrolyte and the high-voltage cathode, resulting in increased overall cell impedance. As already suggested in previous studies [51], the formation of a poly(VC) film on the NMC cathode at high anodic potential values is the most likely explanation for the large improvement in capacity retention (or lifetime) as well as the slight increase of resistance, which may compromise the cell performance at higher discharge rates. Therefore, future studies should be focusing on the investigation and optimization regarding the content of VC. The impact of VC on the parasitic reactions occurring at the cathode could be summarized in a decrease of detrimental electrolyte oxidation reactions at the positive electrode, mainly responsible for the limited lifetime.

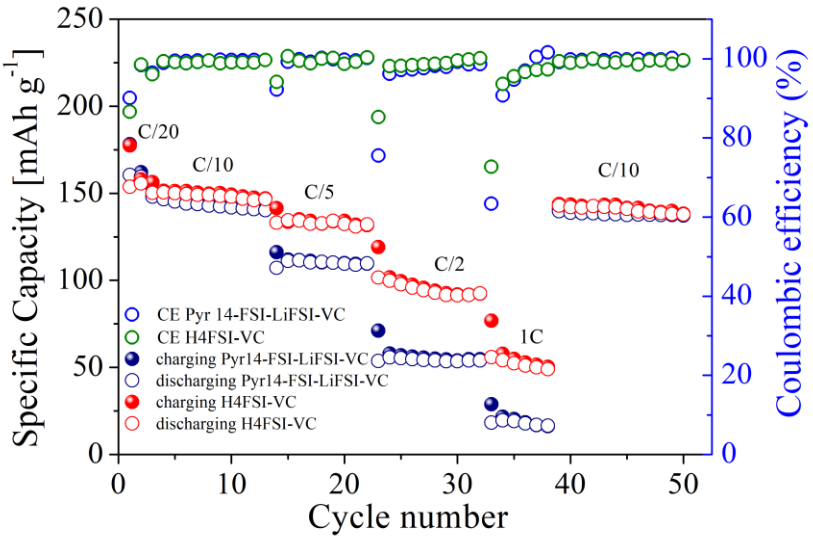

Figure 6. Comparison of the constant-current (galvanostatic) charge/discharge cycling behavior of different [Li metal/IL solution/NMC] cells assembled with H4FSI-VC electrolyte and the corresponding one with the aprotic PYR14FSI-LiFSI-VC: evolution of the specific capacity and the Coulombic efficiency at different C rates with the cycle number.

Furthermore, we compared the performance of PIL/VC-based electrolytes with the corresponding AIL-based electrolytes (either bare or added with VC) in a Li/PYR_{14}FSI-LiFSI/NMC Li metal cell configuration. **Fig. S7** in supplementary data shows comparable electrochemical performance of the PIL/VC and bare AIL based electrolytes at low C/20 and C/10 rates upon initial cycling, while the difference in performance becomes more pronounced moving towards higher C rates: actually, the specific capacity of H_4FSI-VC starts to gradually

drop. The corresponding bare AIL-based cell does not show the same drop in discharge capacity at higher current rates of C/2 and 1C. However, the CE trend and capacity retention upon decreasing the current back to C/10 is extremely improved for the PIL/VC-based electrolyte. This likely accounts for a more stable SEI layer formed by this latter electrolyte compared to the bare AIL-based one. On the other hand, the presence of the protecting layer arising from VC reduction increases the internal resistance and, correspondingly, decreases the rate capability: optimization in this regard is required. It is demonstrated by the comparison in **Fig. 6**, where it can be clearly seen that the addition of VC, particularly at high amounts (10 % by weight in the present work), to the AIL-based electrolyte leads to a remarkable drop in the rate capability of the Li/PYR_{14}FSI-LiFSI-VC/NMC cell. Indeed, Fig. 6 shows the electrochemical performance of the electrolyte solutions based on PIL and AIL, both comprising VC additive. The PIL-VC cell actually outperforms the AIL-VC based counterpart at each of the tested current regimes (enhancement of specific capacity output of the PIL-VC based cell compared to the AIL-VC based counterpart: 4, 15, >40 % at C/20-C/10, C/5, C/2-1C rates, respectively). The results of Fig. 6 clearly demonstrate that, at the same conditions of temperature, current rates, active material loading and amount of VC, PIL-based electrolytes allow superior cycling in lithium metal batteries compared to AILs, particularly at high C-rates. This enlightens how the intrinsic properties of PIL and the lower viscosity affect positively the lithium ion mobility and corresponding cell behaviour. Nonetheless, one should consider that the target of this work is not to compare the performance of PIL and AIL, but demonstrate the positive effects of VC additive when combined with the former. Here, VC was demonstrated to be fundamental to achieve stable cycling in Li metal cells with PILs, remarkably limiting the surface reactivity of PIL-based electrolytes *vs.* the Li metal electrode and, concurrently, enhancing the electrode stability during electrochemical tests, thus foreseeing a bright future for high energy density Li metal and post-Li batteries.

4. Conclusions

In this work, we present the first examples of lab-scale lithium metal cells stable and safely operating with PYR_{H4}^{+}($TFSI^{-}$/FSI^{-})-based protic ionic liquid (PIL) electrolytes, which is accomplished by the use of vinylene

carbonate (VC) encompassed in the PIL-salt solution; exhibiting steady prolonged cycling performace at ambient temperature with both LFP and, even more remarkably, with 4 V class NMC-based cathodes. All the beneficial properties of PILs, in terms of ease of synthesis and cost with respect to AILs, have been matched, with the remarkable outcome of enabling the use of the Li metal anodes, which is characterized by the highest theoretical capacity and lowest electrochemical potential. The electrolytes under investigation, comprised of N-butylpyrrolidinium-($TFSI^-$/FSI^-) based PILs, ($TFSI^-$/FSI^-) based lithium salts and vinylene carbonate (VC) additive, have been tested in Li metal lab-scale cells assembled with LFP and NMC cathodes. The use of VC ensured the formation of a protective layer at the interface between Li metal and the PIL-based electrolytes as well as on the cathode at high anodic potentials, allowing the cells to deliver capacities comparable to those achieved with their AIL-based counterparts.

For sure, to proper engineer the use of PILs with Li metal anode, improvements and optimization are needed, as well as the thorough understanding of several mechanisms within the cell. The protective layer formation and surface chemistry of the Li metal anode before and after cycling, the specific role of FSI^- or $TFSI^-$ anions as well as the interface with high-voltage cathodes; all need to be clarified. Nonetheless, in this work we are demonstrating for the first time that it possible to successfully utilise PIL-based electrolytes also in lithium-metal batteries, and such an initial proof-of-concept represents an important contribution for the realization of cutting-edge, safer, high energy density lithium metal batteries to power next generation electric devices to face the global energy/environmental challenge.

Acknowledgements

M.F. and C.G. acknowledge financial support by the Si-DRIVE Project, which received funding from the EU's Horizon 2020 research and innovation program under GA 814464. The ENABLES project (http://www.enables-project.eu/) received funding from the European Union's Horizon 2020 research and innovation program under Grant Agreement no. 730957.

References

[1] M.Z. Jacobson, M.A. Delucchi, Providing all global energy with wind, water, and solar power, Part I: Technologies, energy resources, quantities and areas of infrastructure, and materials, Energy Policy. 39 (2011) 1154–1169. https://doi.org/10.1016/j.enpol.2010.11.040.

[2] P.J. Loftus, A.M. Cohen, J.C.S. Long, J.D. Jenkins, A critical review of global decarbonization scenarios: What do they tell us about feasibility?, Wiley Interdiscip. Rev. Clim. Chang. 6 (2015) 93–112. https://doi.org/10.1002/wcc.324.

[3] B. Scrosati, J. Garche, Lithium batteries: Status, prospects and future, J. Power Sources. 195 (2010) 2419–2430. https://doi.org/10.1016/j.jpowsour.2009.11.048.

[4] K. Hayashi, Y. Nemoto, S.I. Tobishima, J.I. Yamaki, Mixed solvent electrolyte for high voltage lithium metal secondary cells, Electrochim. Acta. 44 (1999) 2337–2344. https://doi.org/10.1016/S0013-4686(98)00374-0.

[5] Q. Wang, P. Ping, X. Zhao, G. Chu, J. Sun, C. Chen, Thermal runaway caused fire and explosion of lithium ion battery, J. Power Sources. 208 (2012) 210–224. https://doi.org/10.1016/j.jpowsour.2012.02.038.

[6] M. Contestabile, S. Panero, B. Scrosati, Laboratory-scale lithium-ion battery recycling process, J. Power Sources. 92 (2001) 65–69. https://doi.org/10.1016/S0378-7753(00)00523-1.

[7] A. Balducci, S.S. Jeong, G.T. Kim, S. Passerini, M. Winter, M. Schmuck, G.B. Appetecchi, R. Marcilla, D. Mecerreyes, V. Barsukov, V. Khomenko, I. Cantero, I. De Meatza, M. Holzapfel, N. Tran, Development of safe, green and high performance ionic liquids-based batteries (ILLIBATT project), J. Power Sources. 196 (2011) 9719–9730. https://doi.org/10.1016/j.jpowsour.2011.07.058.

[8] D.R. Macfarlane, N. Tachikawa, M. Forsyth, J.M. Pringle, P.C. Howlett, G.D. Elliott, J.H. Davis, M. Watanabe, P. Simon, C.A. Angell, Energy applications of ionic liquids, Energy Environ. Sci. 7 (2014) 232–250. https://doi.org/10.1039/c3ee42099j.

[9] Y. Pu, N. Jiang, A.J. Ragauskas, Ionic Liquid as a Green Solvent for Lignin, J. Wood Chem. Technol. 27 (2007) 23–33. https://doi.org/10.1080/02773810701282330.

[10] P. Kubisa, Ionic liquids as solvents for polymerization processes-Progress and challenges, Prog. Polym. Sci. 34 (2009) 1333–1347. https://doi.org/10.1016/j.progpolymsci.2009.09.001.

[11] M. Watanabe, M.L. Thomas, S. Zhang, K. Ueno, T. Yasuda, K. Dokko, Application of Ionic Liquids to Energy Storage and Conversion Materials and Devices, Chem. Rev. 117 (2017) 7190–7239. https://doi.org/10.1021/acs.chemrev.6b00504.

[12] G.B. Appetecchi, M. Montanino, S. Passerini, Ionic liquid-based electrolytes for high energy, safer lithium batteries, ACS Symp. Ser. 1117 (2012) 67–128. https://doi.org/10.1021/bk-2012-1117.ch004.

[13] M. Moreno, E. Simonetti, G.B. Appetecchi, M. Carewska, M. Montanino, G.-T. Kim, N. Loeffler, S. Passerini, Ionic Liquid Electrolytes for Safer Lithium Batteries, J. Electrochem. Soc. 164 (2017) A6026–A6031. https://doi.org/10.1149/2.0051701jes.

[14] M. Anouti, M. Caillon-Caravanier, Y. Dridi, H. Galiano, D. Lemordant, Synthesis and characterization of new pyrrolidinium based protic ionic liquids. Good and superionic liquids, J. Phys. Chem. B. 112 (2008) 13335–13343. https://doi.org/10.1021/jp805992b.

[15] J. Fuller, A.C. Breda, R.T. Carlin, Ionic liquid-polymer gel electrolytes from hydrophilic and hydrophobic ionic liquids, J. Electroanal. Chem. 459 (1998) 29–34. https://doi.org/10.1016/S0022-0728(98)00285-X.

[16] J.-H. Shin, W.A. Henderson, S. Passerini, PEO-Based Polymer Electrolytes with Ionic Liquids and Their Use in Lithium Metal-Polymer Electrolyte Batteries, J. Electrochem. Soc. 152 (2005) A978. https://doi.org/10.1149/1.1890701.

[17] A. Balducci, R. Dugas, P.L. Taberna, P. Simon, D. Plée, M. Mastragostino, S. Passerini, High temperature carbon-carbon supercapacitor using ionic liquid as electrolyte, J. Power Sources. 165 (2007) 922–927. https://doi.org/10.1016/j.jpowsour.2006.12.048.

[18] R.F. De Souza, J.C. Padilha, R.S. Gonçalves, J. Dupont, Room temperature dialkylimidazolium ionic liquid-based fuel cells, Electrochem. Commun. 5 (2003) 728–731. https://doi.org/10.1016/S1388-2481(03)00173-5.

[19] S. Ferrari, E. Quartarone, P. Mustarelli, A. Magistris, M. Fagnoni, S. Protti, C. Gerbaldi, A. Spinella, Lithium ion conducting PVdF-HFP composite gel electrolytes based on N-methoxyethyl-N-

methylpyrrolidinium bis(trifluoromethanesulfonyl)-imide ionic liquid, J. Power Sources. 195 (2010) 559–566. https://doi.org/10.1016/j.jpowsour.2009.08.015.

[20] T.L. Greaves, C.J. Drummond, Protic ionic liquids: Properties and applications, Chem. Rev. 108 (2008) 206–237. https://doi.org/10.1021/cr068040u.

[21] K. Ghandi, A Review of Ionic Liquids, Their Limits and Applications, Green Sustain. Chem. 04 (2014) 44–53. https://doi.org/10.4236/gsc.2014.41008.

[22] T. Vogl, S. Menne, R.S. Kühnel, A. Balducci, The beneficial effect of protic ionic liquids on the lithium environment in electrolytes for battery applications, J. Mater. Chem. A. 2 (2014) 8258–8265. https://doi.org/10.1039/c3ta15224c.

[23] S. Menne, T. Vogl, A. Balducci, Lithium coordination in protic ionic liquids, Phys. Chem. Chem. Phys. 16 (2014) 5485–5489. https://doi.org/10.1039/c3cp55183k.

[24] S. Menne, J. Pires, M. Anouti, A. Balducci, Protic ionic liquids as electrolytes for lithium-ion batteries, Electrochem. Commun. 31 (2013) 39–41. https://doi.org/10.1016/j.elecom.2013.02.026.

[25] D. Lin, Y. Liu, Y. Cui, Reviving the lithium metal anode for high-energy batteries, Nat. Nanotechnol. 12 (2017) 194–206. https://doi.org/10.1038/nnano.2017.16.

[26] W. Xu, J. Wang, F. Ding, X. Chen, E. Nasybulin, Y. Zhang, J.-G. Zhang, Lithium metal anodes for rechargeable batteries, Energy Environ. Sci. 7 (2014) 513–537. https://doi.org/10.1039/C3EE40795K.

[27] M. Forsyth, G.M.A. Girard, A. Basile, M. Hilder, D.R. MacFarlane, F. Chen, P.C. Howlett, Inorganic-Organic Ionic Liquid Electrolytes Enabling High Energy-Density Metal Electrodes for Energy Storage, Electrochim. Acta. 220 (2016) 609–617. https://doi.org/10.1016/j.electacta.2016.10.134.

[28] P.G. Bruce, S.A. Freunberger, L.J. Hardwick, J.M. Tarascon, LigO2 and LigS batteries with high energy storage, Nat. Mater. 11 (2012) 19–29. https://doi.org/10.1038/nmat3191.

[29] J. Yan, X. Liu, B. Li, Recent progress in Li-rich layered oxides as cathode materials for Li-ion batteries, RSC Adv. 4 (2014) 63268–63284. https://doi.org/10.1039/c4ra12454e.

[30] Christian Julien, Comparative Issues of Cathode Materials for Li-Ions Batteries, Inorganics. 2 (2014) 132–154. https://doi.org/10.3390/inorganics2020132.

[31] D. Aurbach, K. Gamolsky, B. Markovsky, Y. Gofer, M. Schmidt, U. Heider, On the use of vinylene

carbonate (VC) as an additive to electrolyte solutions for Li-ion batteries, Electrochim. Acta. 47 (2002) 1423–1439. https://doi.org/10.1016/S0013-4686(01)00858-1.

[32] H. Ota, Y. Sakata, A. Inoue, S. Yamaguchi, Analysis of Vinylene Carbonate Derived SEI Layers on Graphite Anode, J. Electrochem. Soc. 151 (2004) A1659. https://doi.org/10.1149/1.1785795.

[33] L. Timperman, P. Skowron, A. Boisset, H. Galiano, D. Lemordant, E. Frackowiak, F. Béguin, M. Anouti, Triethylammonium bis(tetrafluoromethylsulfonyl)amide protic ionic liquid as an electrolyte for electrical double-layer capacitors, Phys. Chem. Chem. Phys. 14 (2012) 8199–8207. https://doi.org/10.1039/c2cp40315c.

[34] W.A. Henderson, S. Passerini, Phase behavior of ionic liquid-LiX mixtures: Pyrrolidinium cations and TFSI- anions, Chem. Mater. 16 (2004) 2881–2885. https://doi.org/10.1021/cm049942j.

[35] J. Leys, M. Wübbenhorst, C. Preethy Menon, R. Rajesh, J. Thoen, C. Glorieux, P. Nockemann, B. Thijs, K. Binnemans, S. Longuemart, Temperature dependence of the electrical conductivity of imidazolium ionic liquids, J. Chem. Phys. 128 (2008). https://doi.org/10.1063/1.2827462.

[36] T. Vogl, S. Menne, A. Balducci, Mixtures of protic ionic liquids and propylene carbonate as advanced electrolytes for lithium-ion batteries, Phys. Chem. Chem. Phys. 16 (2014) 25014–25023. https://doi.org/10.1039/c4cp03830d.

[37] S. Menne, T. Vogl, A. Balducci, The synthesis and electrochemical characterization of bis(fluorosulfonyl)imide-based protic ionic liquids, Chem. Commun. 51 (2015) 3656–3659. https://doi.org/10.1039/c4cc09665g.

[38] T. Vogl, S. Passerini, A. Balducci, The impact of mixtures of protic ionic liquids on the operative temperature range of use of battery systems, Electrochem. Commun. 78 (2017) 47–50. https://doi.org/10.1016/j.elecom.2017.04.002.

[39] T. Stettner, S. Gehrke, P. Ray, B. Kirchner, A. Balducci, Water in Protic Ionic Liquids: Properties and Use of a New Class of Electrolytes for Energy-Storage Devices, ChemSusChem. 12 (2019) 3827–3836. https://doi.org/10.1002/cssc.201901283.

[40] J. Ingenmey, S. Gehrke, B. Kirchner, How to Harvest Grotthuss Diffusion in Protic Ionic Liquid Electrolyte Systems, ChemSusChem. 11 (2018) 1900–1910. https://doi.org/10.1002/cssc.201800436.

[41] U.A. Rana, M. Forsyth, D.R. MacFarlane, J.M. Pringle, Toward protic ionic liquid and organic ionic plastic crystal electrolytes for fuel cells, Electrochim. Acta. 84 (2012) 213–222. https://doi.org/10.1016/j.electacta.2012.03.058.

[42] T. Stettner, P. Huang, M. Goktas, P. Adelhelm, A. Balducci, Mixtures of glyme and aprotic-protic ionic liquids as electrolytes for energy storage devices, J. Chem. Phys. 148 (2018). https://doi.org/10.1063/1.5013117.

[43] M. Kerner, N. Plylahan, J. Scheers, P. Johansson, Ionic liquid based lithium battery electrolytes: fundamental benefits of utilising both TFSI and FSI anions?, Phys. Chem. Chem. Phys. 17 (2015) 19569–19581. https://doi.org/10.1039/C5CP01891A.

[44] Y. Dong, J. Demeaux, B.L. Lucht, Investigation of the Effect of Added Methylene Ethylene Carbonate (MEC) and Vinylene Carbonate (VC) on LiNi 0.5 Mn 1.5 O 4 /Graphite Cell Performance , J. Electrochem. Soc. 163 (2016) A2413–A2417. https://doi.org/10.1149/2.1341610jes.

[45] D. Pritzl, S. Solchenbach, M. Wetjen, H.A. Gasteiger, Analysis of Vinylene Carbonate (VC) as Additive in Graphite/LiNi 0.5 Mn 1.5 O 4 Cells , J. Electrochem. Soc. 164 (2017) A2625–A2635. https://doi.org/10.1149/2.1441712jes.

[46] D.M. Piper, T. Evans, K. Leung, T. Watkins, J. Olson, S.C. Kim, S.S. Han, V. Bhat, K.H. Oh, D.A. Buttry, S.H. Lee, Stable silicon-ionic liquid interface for next-generation lithium-ion batteries, Nat. Commun. 6 (2015) 1–10. https://doi.org/10.1038/ncomms7230.

[47] J.R. Nair, F. Colò, A. Kazzazi, M. Moreno, D. Bresser, R. Lin, F. Bella, G. Meligrana, S. Fantini, E. Simonetti, G.B. Appetecchi, S. Passerini, C. Gerbaldi, Room temperature ionic liquid (RTIL)-based electrolyte cocktails for safe, high working potential Li-based polymer batteries, J. Power Sources. 412 (2019) 398–407. https://doi.org/10.1016/j.jpowsour.2018.11.061.

[48] C. Naudin, J.L. Bruneel, M. Chami, B. Desbat, J. Grondin, J.C. Lassègues, L. Servant, Characterization of the lithium surface by infrared and Raman spectroscopies, J. Power Sources. 124 (2003) 518–525. https://doi.org/10.1016/S0378-7753(03)00798-5.

[49] R. Schmitz, R. Ansgar Müller, R. Wilhelm Schmitz, C. Schreiner, M. Kunze, A. Lex-Balducci, S. Passerini, M. Winter, SEI investigations on copper electrodes after lithium plating with Raman

spectroscopy and mass spectrometry, J. Power Sources. 233 (2013) 110–114. https://doi.org/10.1016/j.jpowsour.2013.01.105.

[50] M. Kerner, Pyrrolidinium FSI and TFSI-Based Polymerized Ionic Liquids as Electrolytes for High-Temperature Lithium-Ion Batteries, Batteries. 4 (2018) 10. https://doi.org/10.3390/batteries4010010.

[51] J.C. Burns, N.N. Sinha, D.J. Coyle, G. Jain, C.M. VanElzen, W.M. Lamanna, A. Xiao, E. Scott, J.P. Gardner, J.R. Dahn, The Impact of Varying the Concentration of Vinylene Carbonate Electrolyte Additive in Wound Li-Ion Cells, J. Electrochem. Soc. 159 (2011) A85–A90. https://doi.org/10.1149/2.028202jes.